

Effect of Temperature on Corrosion and Cathodic Protection of X65 Pipeline Steel in 3.5% NaCl Solution

Yingjie Liu, Zhiming Gao*, Xibo Lu, Liqin Wang

School of Material Science and Technology, Tianjin University, Tianjin, 30072, China

*E-mail: gaozhiming@tju.edu.cn

Received: 11 September 2018 / Accepted: 8 November 2018 / Published: 30 November 2018

In this investigation, polarization curve, electrochemical impedance spectroscopy and hydrogen permeation measurements were used to observe the corrosion behavior and cathodic protection of X65 under the influence of temperature. The results show that, with an increase in temperature, I_{corr} increased. E_{corr} decreased and electrochemical impedance decreased, which indicates that corrosion resistance of X65 steel was weakened. As the temperature was increased, D_e decreased and c_0 increased. The defects in X65 steel can block the hydrogen diffusion, but the hydrogen concentration in the specimen increased, which increased the risk of hydrogen embrittlement of X65 steel. As the hydrogen charge potential was shifted negatively, the current density first decreased and then increased, which indicated that the influence of hydrogen air masses in X65 is limited.

Keywords: temperature; X65 pipeline steel; polarization; hydrogen permeation

1. INTRODUCTION

Pipeline steel has been used in the transport of petroleum, petrochemicals, natural gas and water supplies[1]. Due to different service environments, there is always a temperature gradient across different pipe sections, which has a great influence on corrosion behavior[2-4]. A previous study has indicated that temperature has an obvious influence on the limiting diffusion current density[5]. With increases in temperature, the concentration of oxygen and thermal motion of molecules change a lot, which are key factors in corrosion behavior[6]. Yuan[7] has suggested that high temperature increases the corrosion activity of the steel and affects its reaction kinetics. In this work, polarization curve and electrochemical impedance spectroscopy(EIS) measurements were used to analyze the influence of temperature in the range of 20~95°C on X65 steel.

Cathodic protection(CP) is an effective method for long-term protection. However, hydrogen will be produced when the protection potential is too negative, which increases the risk of hydrogen

embrittlement (HE)[8]. The cathodic protection potential is an important parameter for preventing corrosion. Morgan[9] has suggested that cathodic protection criteria should be adjusted negatively with increasing temperature, by approximately 2 mV/°C. Hong[10] analyzed the effect of temperature on current density, which is closely related to cathodic protection design, and suggested that the results at 5°C did not satisfy the CP criteria (-800 mV (SCE)). The main failure mode in cathodic protection is hydrogen embrittlement[11-13]. The susceptibility to hydrogen embrittlement of low alloy and high strength steel will increase as the cathodic protection potential is negatively shifted. In this investigation, the influence of temperature on cathodic protection and hydrogen embrittlement has been studied.

Electrochemical hydrogen permeation measurement is an effective method of observing hydrogen diffusion in steel[14-15], where the diffusible hydrogen concentration, hydrogen permeating flux and hydrogen permeation coefficient can be obtained. Previous investigations have indicated that the polarization potential has significant influence on the hydrogen embrittlement susceptibility of marine steel[16-17]. When the polarization potential is decreased, the number of hydrogen atoms that permeate into the steel increases, which increases the risk of hydrogen embrittlement. In this investigation, the influence of temperature and polarization potential on hydrogen permeation was studied using an improved Devanathan-Stachurski (D-S)[14] cell.

2 EXPERIMENTAL PROCEDURES

2.1 Material and preparation

A 3.5% NaCl solution was used in this work, with a circulating system, as depicted in Fig.1. The samples for electrochemical polarization curve analysis and electrochemical impedance spectroscopy at open circuit potential (OCP) were cut into 10×10×1 mm pieces and embedded with epoxy resin, leaving a working area of 10×10 mm. Samples were then abraded using SiC paper up to 2000 grit. The samples for hydrogen permeation were cut into 40×40×1 mm pieces and abraded up to 2000 grit. All the samples were polished with 0.05 μm grit diamond paste, degreased with anhydrous ethanol, and rinsed with distilled water.

Table 1. Chemical composition of X65 pipeline steel (wt.%)

C	Mn	Si	Cr	P	S	Ni	Cu	Mo
0.05	1.51	0.23	≤0.25	≤0.02	≤0.04	≤0.30	≤0.30	≤0.30

2.2 Polarization curve and electrochemical impedance spectroscopy measurements

Electrochemical measurements are effective ways to analyze the corrosion behavior of metal[18-20]. The measurements were conducted using a PARSTAT 2273 electrochemical workstation with a three-electrode system, where the working electrode (WE) was X65 steel, the reference electrode (RE) was a saturated calomel electrode (SCE), and the counter electrode (CE) was a platinum electrode. The

cathodic polarization curve of X65 steel was obtained from the OCP (vs. SCE) to -0.6 V (vs. OCP), the anodic polarization curve was measured from OCP to 0.5 V (vs. OCP) at a scan rate of 0.1667 mV/s. All the experiments were conducted at 25, 40, 50, 60, 70, 80, 90, and 95 °C using a constant temperature water bath to maintain the required test temperature.

EIS measurements were conducted using a PARSTAT 2273 workstation in a 3.5% NaCl solution with a 10 mV amplitude signal and an applied frequency ranging from 100 kHz to 10 mHz. A three-electrode system was used in these measurements, where the sample was the working electrode, a saturated calomel electrode was the reference electrode with a salt bridge to avoid temperature effects, and a platinum counter electrode was used. All the measurements were performed at OCP, and the data were fitted using ZSimWin software.

2.3 Hydrogen permeation measurement

The electrochemical hydrogen permeation test was carried out using a modified D-S[18] cell, as shown in Fig. 1, with a ZF-100 electrochemical workstation. The specimen was installed between two cells, with a working area of 7.065 mm². Before measurement, a layer of nickel was electrodeposited on the surface of the anodic cell, which was then filled with 0.2 M NaOH. A constant potential of 200 mV was applied to reduce the hydrogen in the specimen. When the background current fell to 1 μA, the hydrogen charging cell was filled with 3.5 % NaCl solution, with a constant potential of -990 mV provided by the ZF-3 potentiostat. The X65 steel specimen was the WE, a SCE with salt bridge was the RE, and a platinum CE was used in the hydrogen charge cell. In the anodic cell, a SCE was the RE and a platinum CE was used.

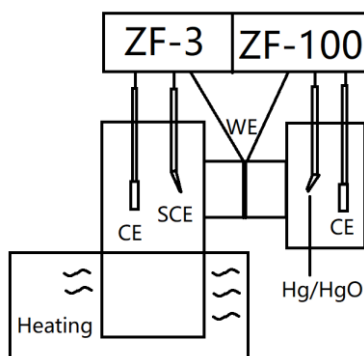


Figure 1. A modified D-S cell for hydrogen permeation at different temperature

3 RESULTS AND DISSCUSION

3.1 Polarization curve and EIS measurements

As is shown in Fig. 2, the Nyquist plots at different temperatures have certain semicircular arcs, which are characterized by the common single-tolerance diagrams. There are straight lines at an angle

of 45 degrees from the x-axis in the low frequency plot, which is characteristic of an electrochemical reaction controlled by diffusion. The plots overlap in the high frequency area, which indicates that the surface conditions of X65 steel are consistent at different temperatures. The corrosion behavior of X65 steel is nearly the same at different temperatures. With increasing temperature, the radius of the impedance arc decreases, which indicates that the increase in temperature accelerates the corrosion reaction and weakens the corrosion resistance of X65.

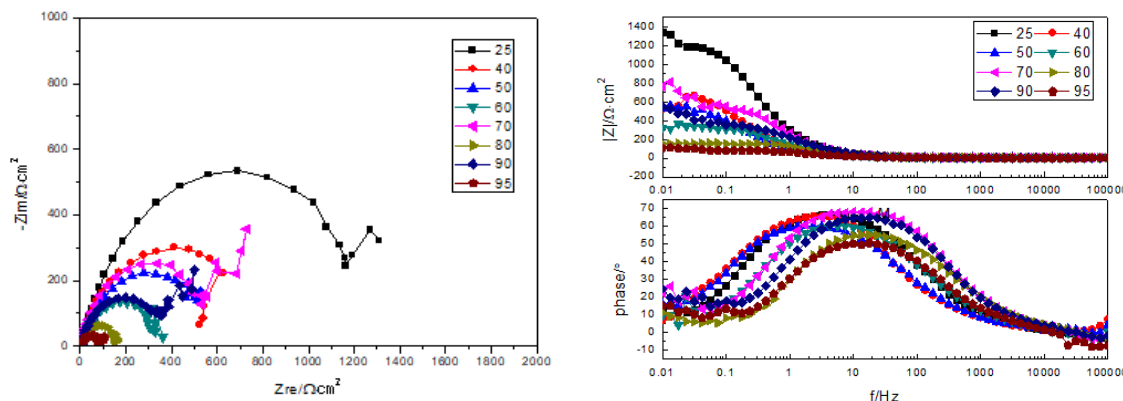


Figure 2. The EIS of X65 steel under open-circuit potential in 3.5% NaCl solution under different temperature (the black curve is 25°C, the red curve is 40°C, the blue curve is 50°C, the green curve is 60°C, the pink curve is 70°C, the dark yellow curve is 80°C, the dark blue curve is 90°C, the brown curve is 95°C)

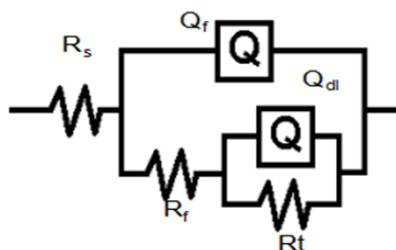


Figure 3. The equivalent circuit of EIS measurement of X65 steel in 3.5%NaCl solution at different temperature

The electrochemical impedance spectroscopy data were fitted with ZSimpWin using the equivalent circuit shown in Fig. 3, and the results are shown in Table 2. The R_s is the solution resistance, while Q_f and R_f are the adsorption capacitance and the resistance of corrosion products, respectively. Q_{dl} refers to the double layer capacitance and R_{ct} refers to the charge transfer resistance. As the temperature was increased, the charge transfer resistance, R_{ct} , decreased. The R_{ct} of X65 steel at 25 °C was 7603 $\Omega \cdot cm^2$, which was 10 times greater than the R_{ct} at 95 °C. This result indicates that the corrosion resistance of X65 steel in a 3.5% NaCl solution decreased as the temperature was increased.

Table 2. The charge transfer impedance(R_{ct}) of X65 steel at different temperature

Temperature/°C	25	40	50	60	70	80	90	95
$R_{ct}/\Omega \cdot cm^2$	7603	4329	2345	1281	1788	1118	765.3	632

The polarization curves in Fig. 4 were obtained at different temperatures in a 3.5% NaCl solution. As Table 2 shows, I_{corr} and E_{corr} were obtained from the polarization curves with a Tafel curve. The cathodic protection potential and hydrogen evolution potential are shown in Table 3.

As the data shows, the I_{corr} of X65 steel increased and the E_{corr} decreased with increasing temperature, which indicates that the corrosion resistance of X65 steel decreased with increasing temperature. These results are in agreement with the EIS results. Furthermore, the limiting diffusion current density increased with increasing temperature, but then decreased above 90 °C. The cause of this phenomenon is the decrease in the concentration of oxygen in solution. Previous study has suggested that with the increase of temperature, the corrosion rate of steel became more severe and the level of localized corrosion rate can be over the average corrosion rate from mass loss measurement[21-23]. In this investigation, I_{corr} increased with the rise of temperature as is shown in Table 3, which indicated that the corrosion rate of X65 increased with the rise of temperature. Meanwhile, the increase of temperature increased the surface activation and promote iron matrix dissolution, which accelerated the corrosive ions permeating into steel. In addition, E_{corr} decreased with increasing temperature, which indicated that the increase in temperature decreased the corrosion resistance of X65 pipeline steel. The results show strong agreement with the results published by several other authors. Pessu[24] studied the effects of CO_2 , H_2S , and temperature on pitting and uniformity of X65 steel in acidic corrosion environments. Temperature was shown to promote pitting of X65 steel and the corrosion products on the surface of X65 steel may further promote the corrosion of X65 steel. Temperature plays an important role in promoting the localized corrosion of X65 steel.

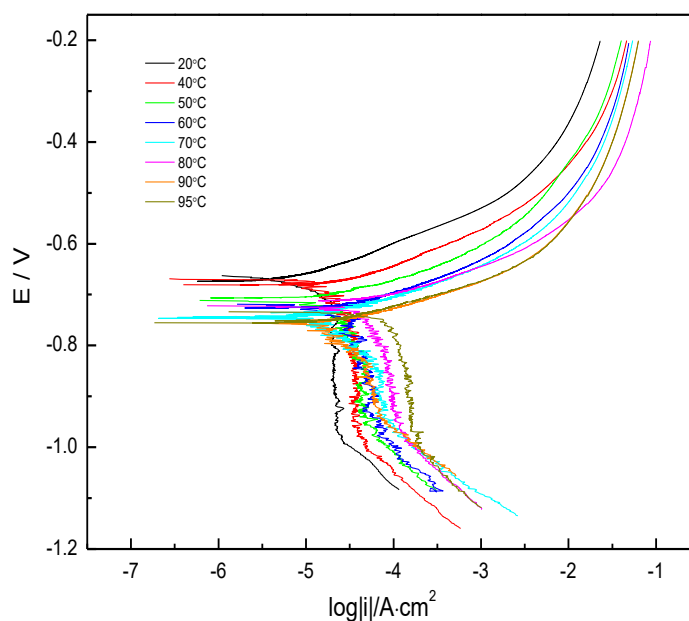


Figure 4. Potentiodynamic polarization curves of X65 steel at different temperature in 3.5% NaCl solution (the black curve is 20°C, the red curve is 40°C, the green curve is 50°C, the dark blue curve is 60°C, the blue curve is 70°C, the pink curve is 80°C, the orange curve is 90°C, the brown curve is 95°C)

Table 3. Corrosion current density and corrosion potential of X65 steel under different temperature by potentiodynamic polarization (vs.SCE)

Temperature/°C	25	40	50	60	70	80	90	95
I_{corr} (A·cm ⁻²)	2.84×10^{-5}	3.40×10^{-5}	3.48×10^{-5}	3.46×10^{-5}	4.80×10^{-5}	7.45×10^{-5}	4.00×10^{-5}	4.95×10^{-5}
E_{corr} (mV)	-673.9	-667.9	-706.6	-726.2	-744.1	-721.8	-755.9	-751.9

According to the Arrhenius equation,

$$\text{Log}(I_{corr}) = \text{Log}(A) - \frac{E_a}{2.303RT} \tag{1}$$

$$\text{Log}\left(\frac{1}{R_{ct}}\right) = \text{Log}(A) - \frac{E_a}{2.303RT} \tag{2}$$

In the equations, R refers to the molar gas constant, and T is the thermodynamic temperature of the 3.5% NaCl solution.

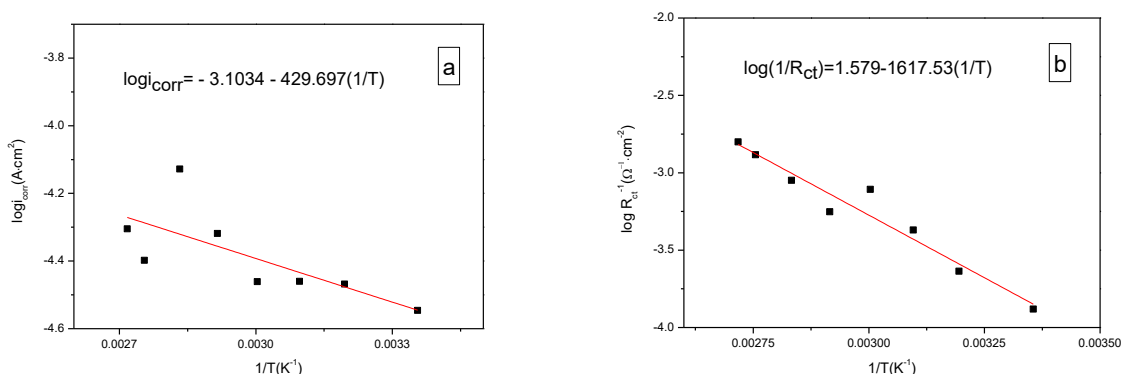


Figure 5. Dependence of I_{corr} and R_{ct} on the temperature according to the Arrhenius plot (a) $\log|I_{corr}| - 1/T$, (b) $\log|R_{ct}| - 1/T$

Table 4. Corrosion current density and corrosion potential of X65 steel in 3.5% NaCl solution under different temperature by Potentiodynamic polarization (mV vs.SCE)

Temperature/°C	25	40	50	60	70	80	90	95
Cathodic protection potential	-800	-820	-850	-870	-900	-930	-910	-920
Hydrogen evolution potential	-950	-960	-965	-970	-978	-980	-974	-976

E_a represents the activation energy of the corrosion reaction and A is a constant. As is shown in Fig. 5, the relation between I_{corr} , R_{ct} , and temperature was fitted to the Arrhenius equation using origin. The activation energy E_a of the corrosion reaction dependent on i_{corr} and R_{ct} was found to be 8.23 kJ·mol⁻¹ and 30.97 kJ·mol⁻¹ respectively. As the plots show, $\log|I_{corr}|$ and $\log|1/R_{ct}|$ followed a linear relationship with $1/T$, which indicated that with increasing temperature, I_{corr} increased and R_{ct} decreased, and the corrosion reaction was accelerated.

Furthermore, the hydrogen evolution potential and cathodic protection potential were obtained using a Tafel curve[25]. As the data shows, the cathodic protection potential of X65 steel reached a value of -820 mV, which is more negative than the potential at 25 °C. These results are not identical with those obtained at room temperature, which suggests that in order to prevent X65 steel from corrosion at high temperature, the cathodic protection potential should be more negative.

3.2 Hydrogen permeation measurement

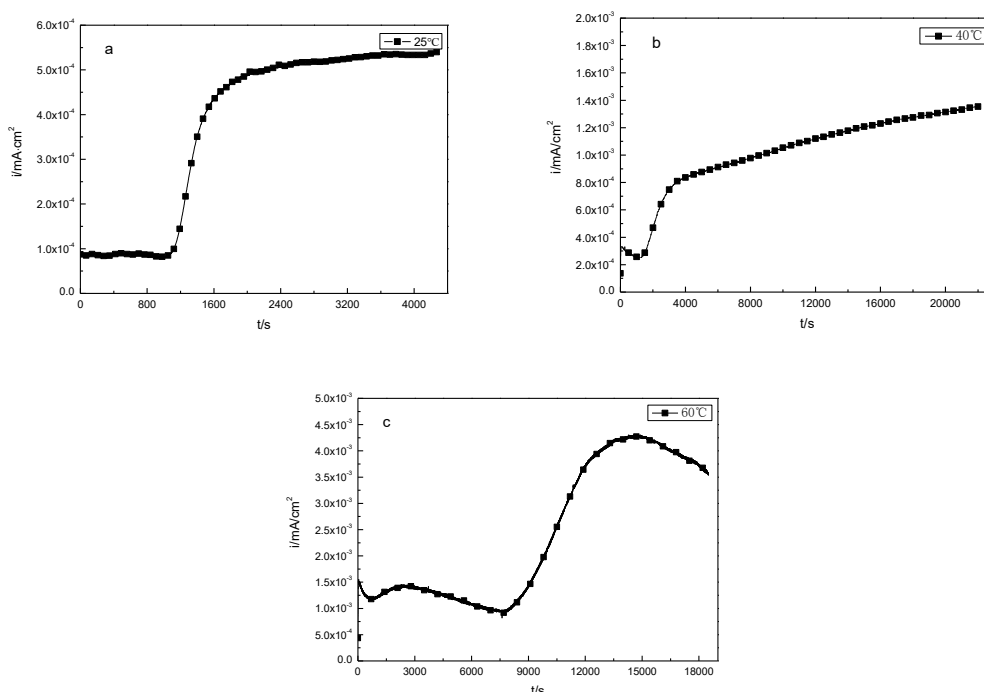


Figure.6 Hydrogen permeation curves of X65 steel under different temperatures (a) (25°C), (b) 40°C, (c) 60°C

Due to the constant cathodic protection potential applied to the specimen, it can be assumed that the hydrogen charging cell generates hydrogen at a uniform rate so that the subsurface hydrogen concentration c_0 is constant. As time goes on, the diffusion flux of hydrogen through the sample to another surface increases, and then the anodic current increases. After a period of time, the diffusion flux of hydrogen to another surface is no longer increasing and the anodic current reaches its maximum point, which is called the steady-state permeation current, recorded as I_{∞} [26] :

$$I_{\infty} = i_{\infty}S \tag{3}$$

Where i_{∞} is the anodic steady-state current density, and S is the working area of the specimen.

According to Fick' first law, the following formula can be written as follows:

$$J_{\infty} = D \frac{c_0}{L} \tag{4}$$

where J_{∞} is the hydrogen permeating flux at steady state. The electric charge generated by 1 mol of hydrogen ions in 1 second is equal to the Faraday constant. So the electric current generated by J mol of hydrogen passing through a unit area in unit time is JF , which is the anodic current density:

$$i = JF \tag{5}$$

We can obtain following formula from the above three formulas :

$$c_0 = \frac{LI_\infty}{DSF} = \frac{LI_\infty}{DS} \times 1.036 \times 10^{-11} \tag{6}$$

Where L is the thickness of the specimen, and D is hydrogen diffusion coefficient, can be calculated bas [27-28]:

$$D = L^2/6t_{0.63} \tag{7}$$

Where $t_{0.63}$ is the lag time of hydrogen permeation, which is the time corresponding to the hydrogen permeation curve at $I(t) / I_\infty = 0.63$.

As the plots show in Fig. 5, the stable diffusion current density was 0.509, 1.345, and 4.3 μ A/cm² at 25, 40, and 60 °C, respectively, which indicates that as the temperature was increased, the steady diffusion current density increased. The diffusible hydrogen concentration (c_0) increased with increasing temperature. As the temperature was increased, more hydrogen was produced, which indicates that the risk of hydrogen embrittlement increased with temperature. Wang[29] has reported that the steady-state permeation current density, diffusion flux of hydrogen and the permeation rate of X52 pipeline steel in wet H₂S environment increased with the rise of temperature, which was almost identical with the results in this investigation. According to the principles of electrochemistry of corrosion, the anodic corrosion equals the cathodic corrosion rate. As the results of polarization curve and EIS measurements shows, corrosion rate increased with the rise of temperature, which means more hydrogen atoms were produced with the increase of temperature. Zhang[30] reported that I_∞ , J_∞ and c_0 presented different variation trends at 293, 298 and 303K under different I regimes, which was the accumulative result of adsorption rate of hydrogen atoms on surface and the acceleration effect on the formation of molecular hydrogen by temperature. In this investigation the temperature was 298, 313 and 333K, the current increased with the rise of temperature, which indicated that the rise of temperature accelerated the hydrogen permeation in X65 steel.

When the temperature was 60°C, the current density decreased after reaching its peak. As the amount of hydrogen dissolved in the X65 steel specimen increased, hydrogen atoms occupied the low energy positions until saturation was reached. Meanwhile defects attracted hydrogen atoms and prevented hydrogen from diffusing into specimen, which resulted in the decrease of the current density. What’s more, corrosion scale can also significantly affect the corrosion process, acting as a diffusion barrier for hydrogen atoms[30]. Under an accumulative result of defects and corrosion scale, the current density decreased after current arriving steady-state current density at 60°C.

Table 4 Calculated results of diffusion flux of hydrogen (J_∞), hydrogen diffusion coefficient (D_e), and diffusible hydrogen concentration (c_0)

Temperature/°C	J_∞ mol/(cm ² ·s)	D_e (cm ² /s)	C_0 (mol/cm ³)
25	5.376x10 ⁻⁶	1.373x10 ⁻⁶	4.147x10 ⁻¹
40	1.394x10 ⁻⁵	4.386x10 ⁻⁷	3.366
60	4.457x10 ⁻⁵	1.756x10 ⁻⁷	26.879

The cathodic reaction of X65 steel is controlled by two reduction reactions of oxygen and hydrogen, which indicates that the hydrogen reduction reaction takes place when the cathodic polarization reaches a certain level. The diffusion coefficient (D_e) of hydrogen in X65 steel is determined by its structure and composition, and the experimental environment. A higher coefficient indicates that more hydrogen can diffuse into the specimen per unit of time. c_0 represents the degree of hydrogen accumulation on the surface of specimen, which reflects the difference in the hydrogen concentration inside and outside the material. As is shown in Table 4, c_0 increases with increasing temperature, which indicates that the reaction activity at high temperature is high and the hydrogen concentration on the surface of X65 steel is high. However, D_e decreased with increasing temperature, which was mainly caused by defects in the specimen. There was a certain amount of hydrogen atoms in X65 steel, which occupied the low energy positions. As the temperature increased, the whole system was in an active state, and a large amount of hydrogen was produced. Therefore, more hydrogen atoms reached into the specimen, which were attracted by hydrogen in low energy positions and formed an air mass. When the rest of the hydrogen atoms diffused across the specimen, this air mass would block the diffusion, which resulted in the decrease of D_e of hydrogen in X65 steel.

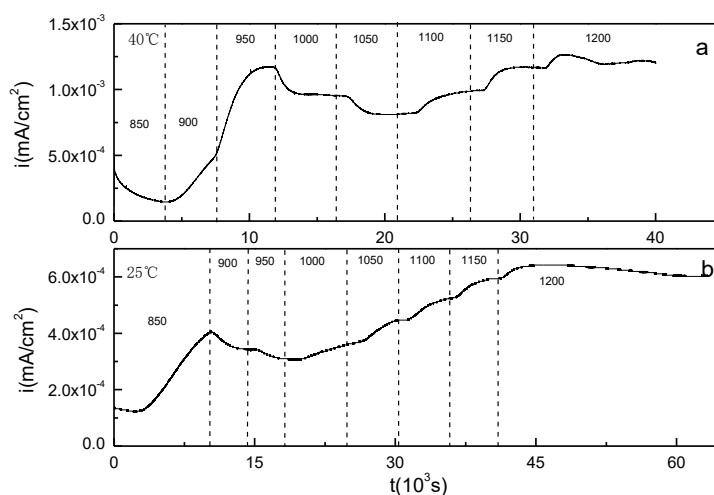


Figure 7. Hydrogen permeation curves of X65 steel under different temperatures with different cathodic potentials (a) 40°C, (b) 25°C

In order to analyze the relation between hydrogen permeation potential and temperature, continually-varied potential hydrogen permeation measurements were conducted using the ZF-100 system and a potentiostat. As Fig.7 shows, the hydrogen permeation potential was about -850 mV at 25°C and -900 mV at 40°C, which indicates that the increase of temperature leads to the decrease of hydrogen evolution potential. As the hydrogen charge potential shifted negatively, i_{∞} at different temperature decreased firstly and then increased as is shown in Table 6 and Table 7, which indicated that hydrogen formed air mass and prevented the diffusion of hydrogen in X65 steel. Because the amount of air mass was limited, the blocking effect was eventually broken. After -1000mV at 25°C and 1050mV in 40°C, current density increased with the decrease of potential. Furthermore, the influence of the environment on hydrogen permeation is complicated; besides temperature, the surface state and structure of the material are also key factors in hydrogen permeation. Zhang[31] analyzed hydrogen diffusivity

and the sub-surface concentration of hydrogen in three pipeline steels using high-pressure hydrogen permeation and electrochemical hydrogen permeation tests in simulated seawater. The results were almost identical with the results obtained in this investigation. Lattice defects (vacancies, dislocations, grain boundaries) provide a variety of trapping sites, which absorbed hydrogen atoms and affected the diffusion of hydrogen atoms. However, the amount of defects in X65 steel is limited. It was obvious that the decrease of potential promoted the hydrogen permeation of pipeline steel and increased the risk of hydrogen embrittlement, and sub-surface hydrogen concentration of X65 increased with the decrease of polarization potential.

Table 6. Stable diffusion current density i_{∞} at different hydrogen charge potential at 25°C

Potential(mV)	-900	-950	-1000	-1050	-1100	-1150	-1200
$i_{\infty}(10^{-3}\mu\text{A}\cdot\text{cm}^2)$	0.40	0.31	0.37	0.45	0.53	0.59	0.61

Table 7. Stable diffusion current density i_{∞} at different hydrogen charge potential at 40°C

Potential(mV)	-900	-950	-1000	-1050	-1100	-1150	-1200
$i_{\infty}(10^{-3}\mu\text{A}\cdot\text{cm}^2)$	0.52	1.17	0.96	8.10	1.01	1.20	1.26

4. CONCLUSIONS

In order to study the influence of temperature on corrosion behavior and hydrogen permeation, polarization curve, EIS and hydrogen permeation measurements were conducted in a 3.5% NaCl solution at different temperatures. The conclusions are summarized as follows.

(1) With increasing temperature, I_{corr} increased, E_{corr} decreased, and the electrochemical impedance decreased, which indicates that the corrosion resistance of X65 steel decreased. In order to protect material from corrosion, the temperature must be controlled at a low level.

(2) As the temperature was increased, D_e decreased and c_0 increased. The defects in X65 steel block hydrogen diffusion, but the hydrogen concentration in the specimen increased, which was the accumulated result of the adsorption rate of hydrogen atoms on the surface and the acceleration of the formation of molecular hydrogen due to the higher temperature. The increased temperature increases the risk of hydrogen embrittlement of X65 steel.

(3) As the hydrogen charge potential was shifted negatively, the current density first decreased and then increased. There is a critical value of hydrogen air mass, and i_{∞} increased after the hydrogen atoms in X65 steel reached this value, and the sub-surface hydrogen concentration of X65 increased with decreasing polarization potential.

ACKNOWLEDGEMENTS

This research is supported by National Natural Science Foundation of China (No.51371124, No.51671144,), the Major State Basic Research Development Program (973 Program) (Granted No. 2014CB046805), Supporting Plan Project of Tianjin City (16YFZCGX00100), and Natural Science Foundation of Tianjin (No.17JCTPJC47100).

References

1. B.A. Shaw, R.G. Kelly, *Electrochem. Soc. Interface*, 15 (2006) 24.
2. L. He, X.Y. Liu, X.C. Song, M. Feng, Z.Y. Zhao, *Corros. Prot.*, 38 (2017) 391.
3. Y. F. Cheng, F. R. Steward, *Corros. Sci.*, 46 (2004) 2405.
4. C.F. Chen, M.X. Lu, G.X. Zhao, Z.Q. Bai, M.L. Yan, Y.Q. Yang, *Acta Metal. Sin.*, 8 (2003) 391.
5. M. Gong, M. Feng, Y. Zhang, G.H. Zhang, *Corros. Prot.*, 32 (2011) 691.
6. F.E. Varela, Y. Kuratat, N. Sanada, *Corros. Sci.*, 39 (1997) 775.
7. W. Yuan, F. Huang, J. Liu, *Corros. Eng., Sci. Technol.*, 53 (2018) 393.
8. R. Thodla, M.T. Piza Paes, B. Gerst, *Int. J. Hydrogen. Energy.*, 40 (2015) 17051.
9. J. Morgan, M. NACA., (1993) 102.
10. Hong M.S, Hwang J.H, Kin J.H, *Corrosion*, 74 (2018) 123.
11. D. Figueroa, M.J. Robinson, *Corros. Sci.*, 52 (2010) 1593.
12. D. Figueroa, M.J. Robinson, *Corros. Sci.*, 50 (2008) 1066.
13. M. Wang, E. Akiyama, K. Tsuzaki, *Mater. Sci. Eng.*, 398 (2005) 37.
14. T. Boiadjeva, L. Mirkova, H. Kronberger, T. Steck, M. Money, *Electrochim. Acta*, 114 (2013)790.
15. Y. Kyo, A.P. Yadav, A. Nishikata, T. Tsuru, *Corros. Sci.*, 53 (2011) 3043.
16. T.M. Zhang, W.M. Zhao, W. Guo, Y. Wang, *Corros. Prot.*, 34 (2014) 315.
17. L. Zhang, M. Du, J.F. Liu, Y. Li, P.L. Liu, *Mater. Sci. Technol.*, 19 (2011) 96.
18. S.B. Wu, J.Q. Wang, S.Z. Song, D.H. Xia, Z.M. Zhang, Z.M. Gao, J.H. Wang, W.X. Jin, W.B. Hu, *J. Electrochem. Soc.*, 164 (2017) 94.
19. D.H. Xia, J.Q. Wang, Z. Wu, Z.B. Qin, L.K. Xu, W.B. Hu, Yashar Behnamian, J.L. Luo, *Sens. Actuators, B*, 280 (2018) 235.
20. Y.H. Sun, S.B. Wu, D.H. Xia, L.K. Xu, J.Q. Wang, S.Z. Song, H.Q. Fan, Z.M. Gao, J. Zhang, Z. Wu, W.B. Hu, *Corros. Sci.*, 140 (2018) 260.
21. Y. Hua, R. Barker, A. Neville, *Int. J. Greenh. Gas. Con.*, 31 (2014) 48.
22. N.Y. Zhang, D.Z. Zeng, Z.M. Yu, W.T. Zhao, J.Y. Hu, W.L. Deng, G. Tian, *Int. J. Electrochem. Sci.*, 13 (2018) 4489.
23. L. Zhang, X. Tang, Z. Wang, T. Li, Z.R. Zhang, M.X. Lu, *Int. J. Electrochem. Sci.*, 12 (2017) 8806.
24. F. Pessu, R. Barker, A. Neville, *Corrosion.*, 73 (2017) 1168.
25. C.N. Cao, Chemical Industry Press, (2008) 77 Beijing, China.
26. Q. Chu, J.X. Li, Hydrogen embrittlement and stress corrosion, (2013) Beijing, China.
27. E. Fallahmohammadi, F. Bolzoni, L. Lazzari, *Int. J. Hydrogen. Energy.*, 38 (2013) 2531.
28. Y.F. Cheng, *Int. J. Hydrogen. Energy*, 32 (2007) 1269.
29. Z. Wang, M.L. Liu, M.X. Lu, L. Zhang, J.Y. Sun, Z.R. Zhang, X. Tang, *Int. J. Electrochem. Sci.*, 13 (2018) 915.
30. L. Zhang, W.H. Cao, K.D. Lu, Z. Wang, Y.Y. Xing, Y.X. Du, M.X. Lu, *Corros. Sci.*, 42 (2017) 3389.
31. T.M. Zhang, W.M. Zhao, T.T. Li, Y.J. Zhao, Q.S. Deng, Y. Wang, W.C. Jiang, *Corros. Sci.*, 131 (2018) 104.